A MODIFIED T-VALUE METHOD FOR SELECTION OF STRAIN GAGES FOR MEASURING LOADS

Ming H. Tang

NASA Dryden Flight Research Center
Edwards, California

To be presented at
Fall Meeting of the Western Regional Strain Gage Committee
Society for Experimental Stress Analysis
Naval Weapons Center, China Lake, California
September 16 and 17, 1980

F80-0219

A MODIFIED T-VALUE METHOD FOR SELECTION OF STRAIN GAGES FOR MEASURING LOADS

Ming H. Tang
Dryden Flight Research Center
Edwards, California

ABSTRACT

This paper examines a modified T-value method for selection of strain gages for measuring loads on a low-aspect-ratio multispar wing. Shear, bending moment, and torque equations derived using the modified T-value method are used to compute loads from three applied load distributions. The results are compared with loads computed by equations derived using the T-value method.

INTRODUCTION

Calibrated strain gages are extensively used to measure aircraft loads in flight, particularly on lifting surfaces. The prevailing calibration method (ref. 1) is based on the fact that, although the stress in structural members may not be a simple function of shear, bending moment, or torque, it is possible to combine the responses of selected strain gages to provide a measure of each parameter.

The method works well for high-aspect-ratio structures where load paths from the wing to fuselage are few and well defined. However, for high speed flight, the emergence of low-aspect-ratio delta wing structures with redundant multispars made load measurement with strain gages more difficult. Typical of this type of structure are the M2-F2 outboard fin (fig. 1) and the YF-12 wing (fig. 2). Refinements to the basic method for measuring loads on low-aspect-ratio structures are given in references 2 to 4.

In general, low-aspect-ratio multispar structures are extensively instrumented with strain gages to assure that critical load paths are monitored for reliable load measurement. The key strain gages are selected based on the responses from the calibration. One technique for selecting the appropriate strain gages for measuring loads is the T-value method, described in references 2 and 4.

This paper presents a special adaption of the T-value method which includes three additional parameters for weighing the relative merits of each strain-gage bridge in a load equation. These parameters are (1) the relative magnitude of the strain-gage responses, (2) the gage-to-load correlation, and (3) the gage-to-gage intercorrelation.

The performances of the load equations derived from both the T-value and the modified T-value, MT-value, methods were demonstrated at room temperature condition. Three distributed loads were applied to a wing test structure. The resulting strain-gage responses were used in both the T-value and the MT-value derived equations to calculate shear, bending moment, and torque loads. These values were then compared with the actual applied loads.

SYMBOLS

L	generalized load (shear, bending moment, or torque)
MT	modified T-value
T	T-value
x	Cartesian coordinate in chord direction
y	Cartesian coordinate in span direction
β	constant in load equation
γ	coefficient of the intercorrelation between a strain-gage bridge response and all other strain-gage bridge responses to calibration loads
λ	coefficient of the correlation between the strain-gage bridge response and the calibration loads
μ	nondimensional strain-gage bridge response
$\bar{\mu}$	mean absolute magnitude of μ
ε	standard error of β

Subscripts:

$1, 2, 3, \ldots, j$	order of the appearance of terms in load equation
i	discrete function

TEST STRUCTURE

Results from a large number of hypersonic cruise aircraft studies, in particular, references 5 to 7, led to the design and construction of the hypersonic wing test structure shown in figure 3. The test structure represents the primary wing box of a multispar low-aspect-ratio wing designed for hypersonic cruise at Mach 8. The test structure is primarily constructed of René 41 and has a planform area of 7.9 square meters (85 square feet). The six spars are spaced 50.8 centimeters (20 inches) apart and are covered by spanwise-stiffened beaded panels and chordwise-stiffened beaded heat shields. A more complete description of the hypersonic wing test structure is given in references 8 and 9.

INSTRUMENTATION

The load measurement instrumentation on the hypersonic wing test structure consisted of 12 four-active-arm strain-gage bridges. The general locations of the

strain-gage bridges and the calibration load points are shown in figure 4.

Six bending bridges (numbers 104, 304, 504, 704, 904, and 1104) and six shear bridges (numbers 105, 305, 505, 705, 905, and 1105) were installed on the caps and webs of the six spars respectively.

CALIBRATION

The strain-gage bridges were calibrated at room temperature for measuring shear, bending moment, and torque using the point-by-point procedure of reference 1. A tension load of 8896 Newtons (2000 pounds) was applied at each of the 18 load points on the hypersonic wing test structure shown in figure 4.

The accuracy of the data acquisition system for strain-gage measurements was estimated to be ±4.88 microstrain, which represents 0.3 percent of the strain-gage calibrate output. A more complete description of the loading tests is given in reference 9.

LOAD EQUATIONS

The multiple linear regression method described in reference 1 was used to derive shear, bending moment, and torque equations for determining loads on the test structure. Initially, all 12 strain-gage bridges were utilized to relate the applied calibration loads to the bridge responses. The generalized load equation is as follows:

$$L = \beta_1\mu_1 + \beta_2\mu_2 + \beta_3\mu_3 + \ldots + \beta_j\mu_j \tag{1}$$

where L is the applied load, β is the load equation constant, and μ is the nondimensional strain-gage bridge response. An analysis of the loads calibration is given in reference 8.

T-Value Method

One method (refs. 2 and 4) for reducing the number of bridges in equation (1) is to use the T-value as a measure of the bridge relevancy. The T-value is defined as follows:

$$T_i = \frac{\beta_i}{\varepsilon_i} \tag{2}$$

where T is the T-value weighing the relevancy of the ith strain-gage bridge, β_i is the equation constant, and ε_i is the standard error of β_i.

The number of bridges in the load equation is successively reduced by eliminating the bridge with the smallest T-value. Each time a bridge is eliminated, a new equation is derived from the remaining bridges and new T-values are calculated. The procedure is repeated until a set of equations varying from 12 terms to 2 terms is derived.

Modified T-Value Method

In order to improve the selection of appropriate strain gages for load equations, the T-value method was modified to include the relative magnitude of the strain-gage responses, the gage-to-load correlation, and the gage-to-gage intercorrelation factors. This modified T-value, MT-value, is defined as follows:

$$MT_i = \frac{\bar{\mu}_i \lambda_i \beta_i}{\gamma_i \varepsilon_i} \tag{3}$$

where MT_i is the modified T-value weighing the relevancy of the ith strain-gage bridge, $\bar{\mu}_i$ is the mean absolute magnitude of the nondimensional strain-gage bridge response to calibration loads, λ_i is the coefficient of the correlation between the strain-gage bridge response and the calibration loads, β_i is the equation constant, γ_i is the coefficient of the correlation between the strain-gage bridge response with respect to all other bridge responses to calibration loads, and ε_i is the standard error of β_i.

The absolute magnitude of the gage response, $\bar{\mu}$, is important in that large $\bar{\mu}$ will cause the resolution error of the gage to be less significant than another gage with small $\bar{\mu}$ in the load equation.

On a multispar structure with redundant load paths (figs. 1 to 3), a strain-gage bridge may be highly responsive to loads on the spar to which the gage is attached but not sensitive to loads on remote spars. The gage-to-load correlation coefficient, λ, is introduced in the MT-value to account for this behavior. Large λ indicates good sensitivity to most of the applied calibration loads and thus should be retained in the load equation.

The magnitude of the gage-to-gage- intercorrelation coefficient, γ, reflects the redundancy of a gage with respect to the remaining gages in the load equation. Here, small γ is desirable, for it indicates uniqueness of the gage in measuring loads.

The terms $\bar{\mu}$, β, λ, and ε are calculated as part of the statistical information in the multiple linear regression computer program used in deriving the load equation constants given in reference 10. The term γ is calculated from the strain-gage intercorrelation matrix as described in reference 11.

Equation Influence Coefficients

Influence coefficient plots (figs. 5 and 6) of complete load equations for determining shear, bending moment, and torque give a graphic illustration of the nature of the equation. (The plots are computed using the procedure described in reference 12.)

Ideally, the shear equation influence coefficient plot should appear as a line of zero slope. The lack of response to spanwise variation indicates no sensitivity to bending, and at any given span location no variation of data points with changes in chord location indicates insensitivity to torque. Similarly, the ideal bending moment equation plot should be a straight line of constant slope. And finally, the ideal torque equation plot should assume the planform of the load points. Figure 5 shows the influence coefficient plots for equations derived by eliminating bridges with the T-value method. The equations derived with the modified T-value method are shown in figure 6. In general, the shapes of the equation influence coefficient plots deviate from the ideal pattern as the number of terms in the equation are reduced from 12 to 2, thereby indicating a degradation in performance.

PERFORMANCE OF LOAD EQUATIONS

The purpose of a load equation is to accurately calculate flight loads. Therefore, rather than rely on statistical information generated by the calibration loads, the comparative assessment of the T and MT sets of equations is based on the accuracy of measurement of three distributed loads applied independently of the point-by-point calibration.

The three distributed loads applied at room temperature, which are shown in figure 7, represent the aerodynamic loads on a wing during subsonic, supersonic, and maneuvering flight as described in reference 13.

Figure 8(a) compares the T and MT derived shear equation values for the three distributed loads. Reducing the number of bridges from 12 to 2 results in a deviation of the computed shear from the applied load for both sets of shear equations. However, the MT derived shear equations are consistently more accurate than the T derived shear equations. The improved measurement is most evident for equations containing six bridges or less.

Figure 8(b) compares the performance of the T and MT derived bending moment equations. The same trend exists in bending as for shear and the improved accuracy is again most apparent for equations containing six bridges or less.

The T and MT derived torque equation performance is shown in figure 8(c). Again, the improvement of the MT derived equation measurement of torque is evident. The improvement is most evident for equations containing five bridges or less. However caution must be exercised when examining torque data because the quantities are dependent on the location of the torque reference axis.

A complete tabulation of the percent difference between the computed and applied shear, bending moment, and torque for both the T and the MT sets of equations is given in reference 10.

CONCLUDING REMARKS

The two sets of load equations, derived by both the T-value and the MT-value methods, permitted a direct comparison of the relative accuracies of the two sets of equations in computing the values of the distributed loads.

The MT-value derived equations proved to be consistently more accurate than the T-value derived equations in computing the values of the three load distributions. In general, the improved accuracy was most notable for equations containing six bridges or less.

The MT-value method provides a systematic, formalized approach to reducing the large number of strain gages used in a load equation for a multispar structure. The concept was experimentally demonstrated on the hypersonic wing test structure; however, the MT-value method should be applied prudently to other structures until universal applicability is verified.

REFERENCES

1. Skopinski, T. H.; Aiken, William S., Jr.; and Houston, Wilbur B.: Calibration of Strain-Gage Installations in Aircraft Structures for Measurement of Flight Loads. NACA Rept. 1178, 1954.

2. Hovell, P. B.; Webber, D. A.; and Roberts, T. A.: The Interpretation of Strain Measurements for Flight Load Determination. C. P. No. 839, British A. R. C., 1966.

3. Hovell, P. B.; Webber, D. A.; and Roberts, T. A.: The Use of Calibrated Strain Gauges for Flight Load Determination. C. P. No. 1041, British A. R. C., 1969.

4. Sefic, Walter J.; and Reardon, Lawrence F.: Loads Calibration of the Airplane, NASA YF-12 Loads Program. NASA TM X-3061, 1974, pp. 61-107.

5. Plank, P. P.; Sakata, I. F.; Davis, G. W.; and Richie, C. C.: Substantiation Data for Hypersonic Cruise Vehicle Wing Structure Evaluation. NASA CR-66897, (Vols. I to III), 1970.

6. Plank, P. P.; Sakata, I. F.; Davis, G. W.; and Richie, C. C.: Hypersonic Cruise Vehicle Wing Structure Evaluation. NASA CR-1568, 1970.

7. Plank, P. P.; and Penning, F. A.: Hypersonic Wing Test Structure Design, Analysis, and Fabrication. NASA CR-127490, 1973.

8. Tang, Ming H.; and Fields, Roger A.: Analysis of a Loads Calibration of a Hypersonic Cruise Wing Test Structure. Proceedings of the Western Regional Strain Gage Committee, Sept. 1977, Soc. for Experimental Stress Anal., pp. 11-18.

9. Fields, Roger A.; Reardon, Lawrence F.; and Siegel, William H.: Loading Tests of a Wing Structure for a Hypersonic Aircraft. NASA TP-1596, 1980.

10. Tang, Ming H.; and Sheldon, Robert G.: A Modified T-Value Method for Selection of Strain Gages for Measuring Loads on a Low Aspect Ratio Wing. NASA TP-1748, 1980.

11. Anderson, Theodore W.: Introduction to Multivariate Statistical Analysis. John Wiley & Sons, Inc., 1958. pp. 86-89.

12. Jenkins, Jerald M.; Kuhl, Albert E.; and Carter, Alan L.: Strain Gage Calibration of a Complex Wing. AIAA J. Aircraft, vol. 14, no. 12, Dec. 1977, pp. 1192-1196.

13. Jenkins, Jerald M. and Kuhl, Albert E.: A Study of the Effect of Radical Load Distributions on Calibrated Strain Gage Load Equations. NASA TM-56047, 1977.

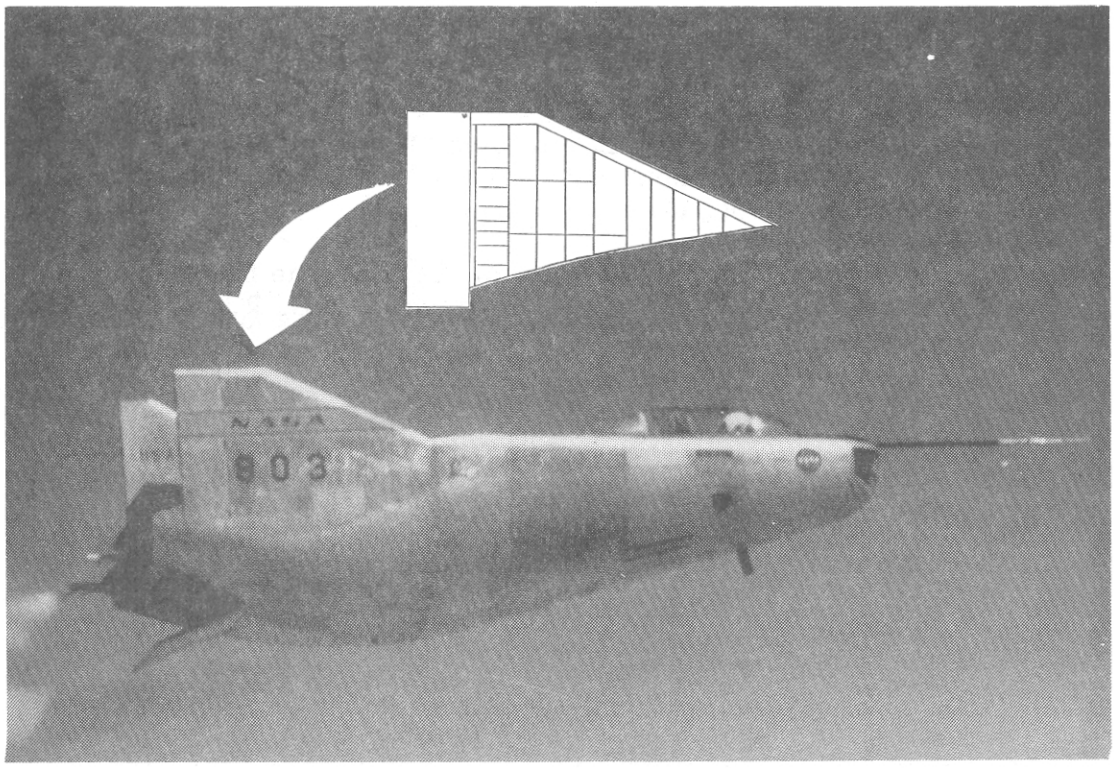

Figure 1. M2-F2 lifting body vehicle and outboard fin.

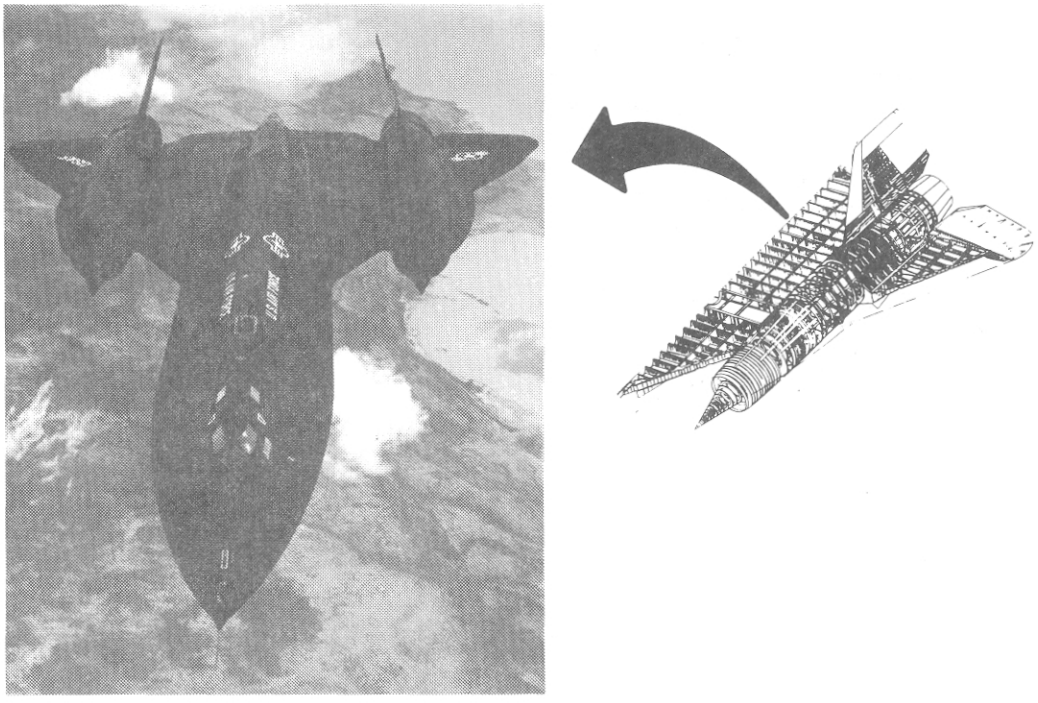

Figure 2. YF-12A airplane and wing.

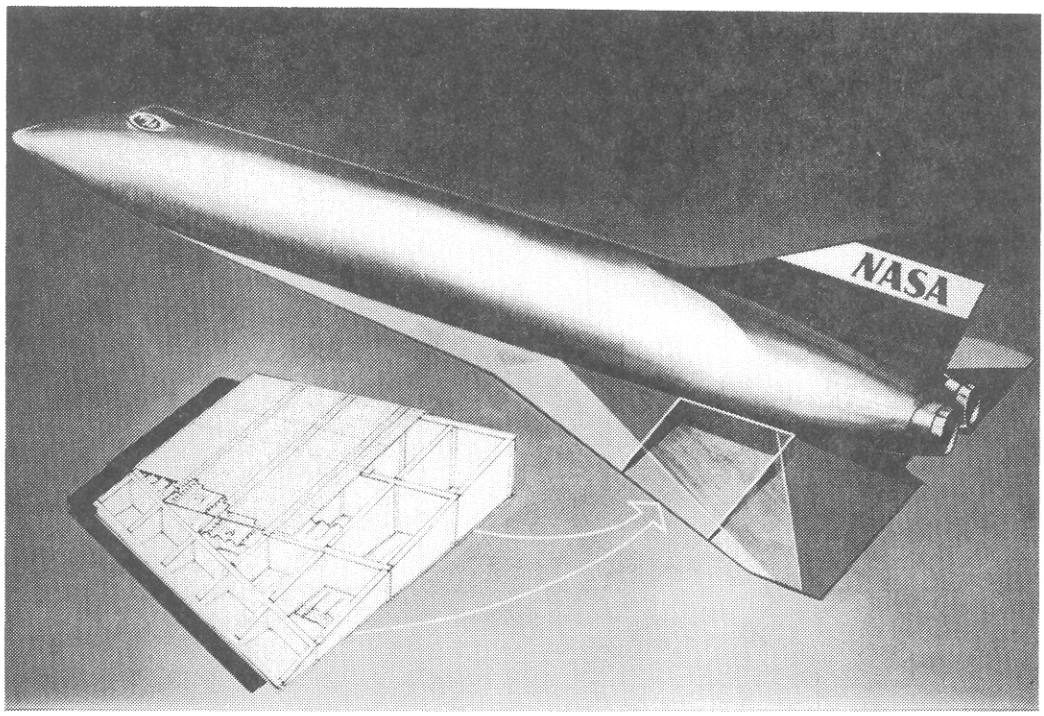

Figure 3. Hypersonic research airplane and hypersonic wing test structure.

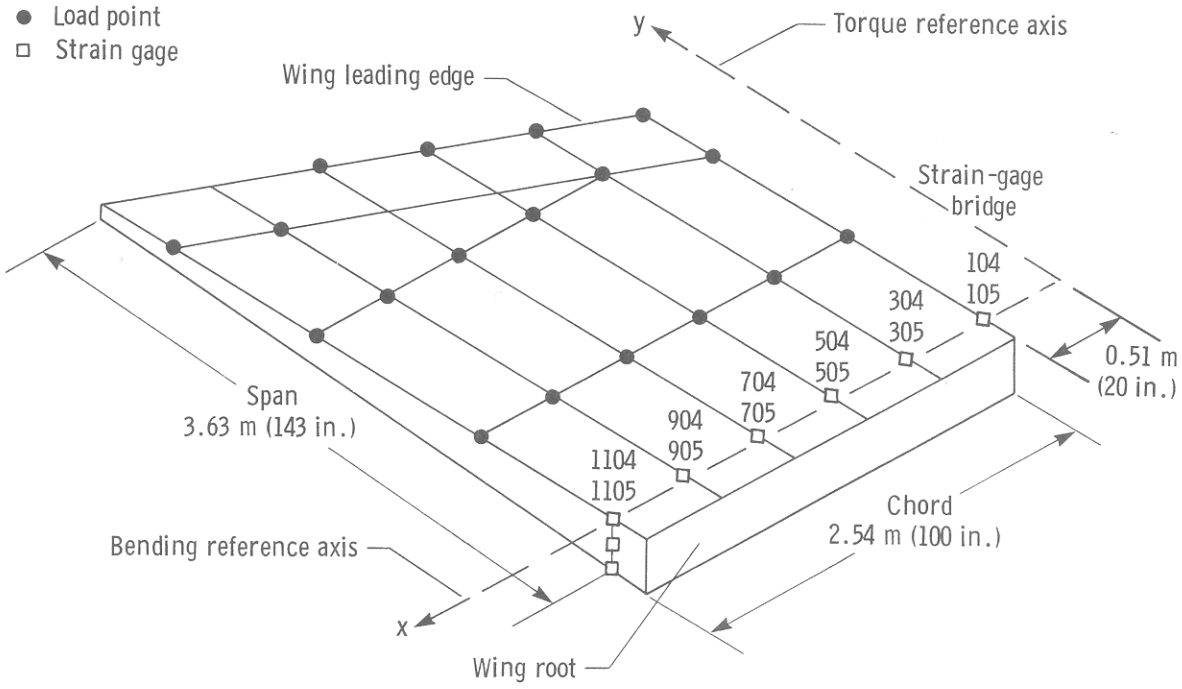

Figure 4. Strain-gage bridge locations and calibration load points on the hypersonic wing test structure.

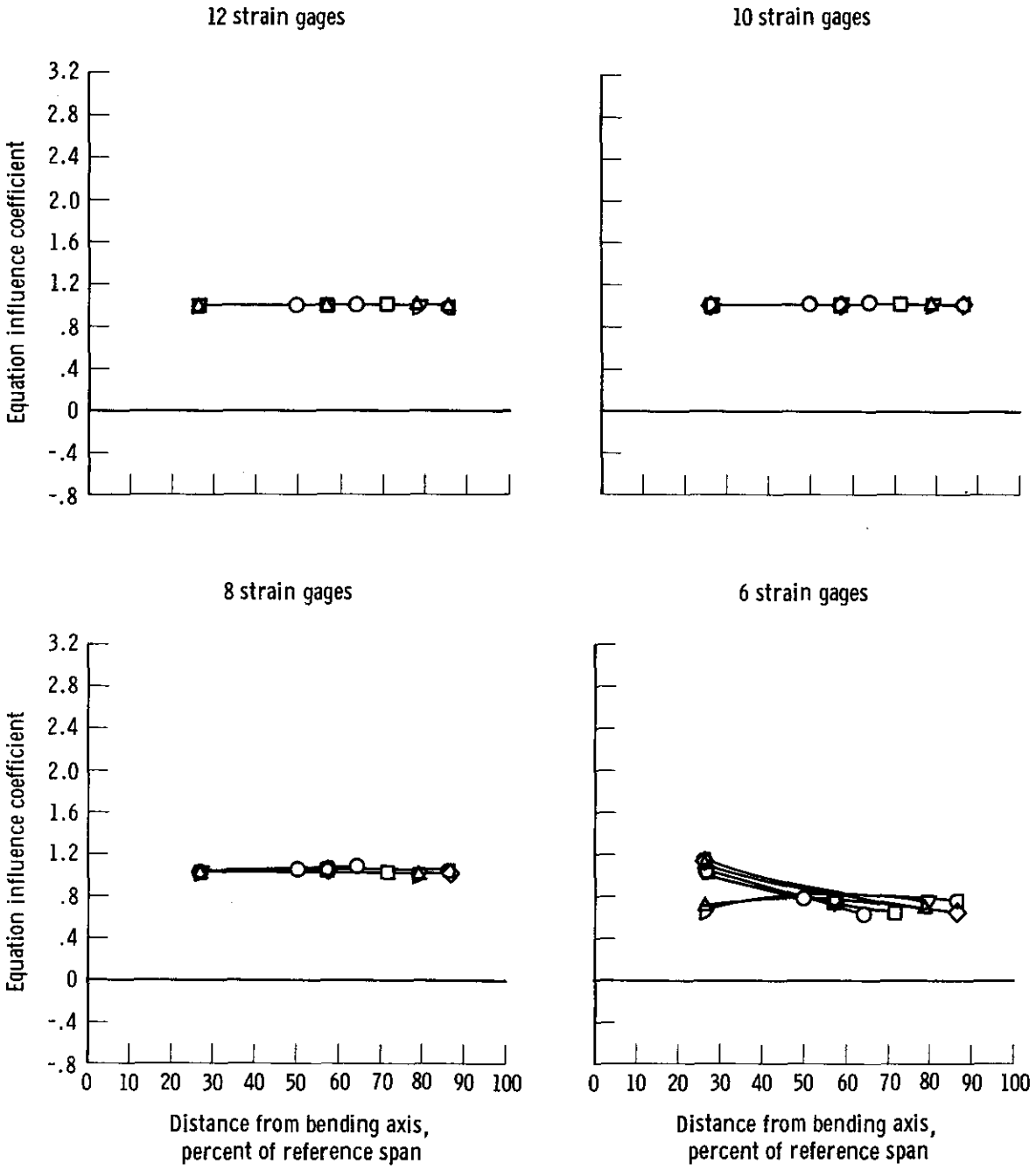

(a) Shear.

Figure 5. T-value derived equation influence coefficient.

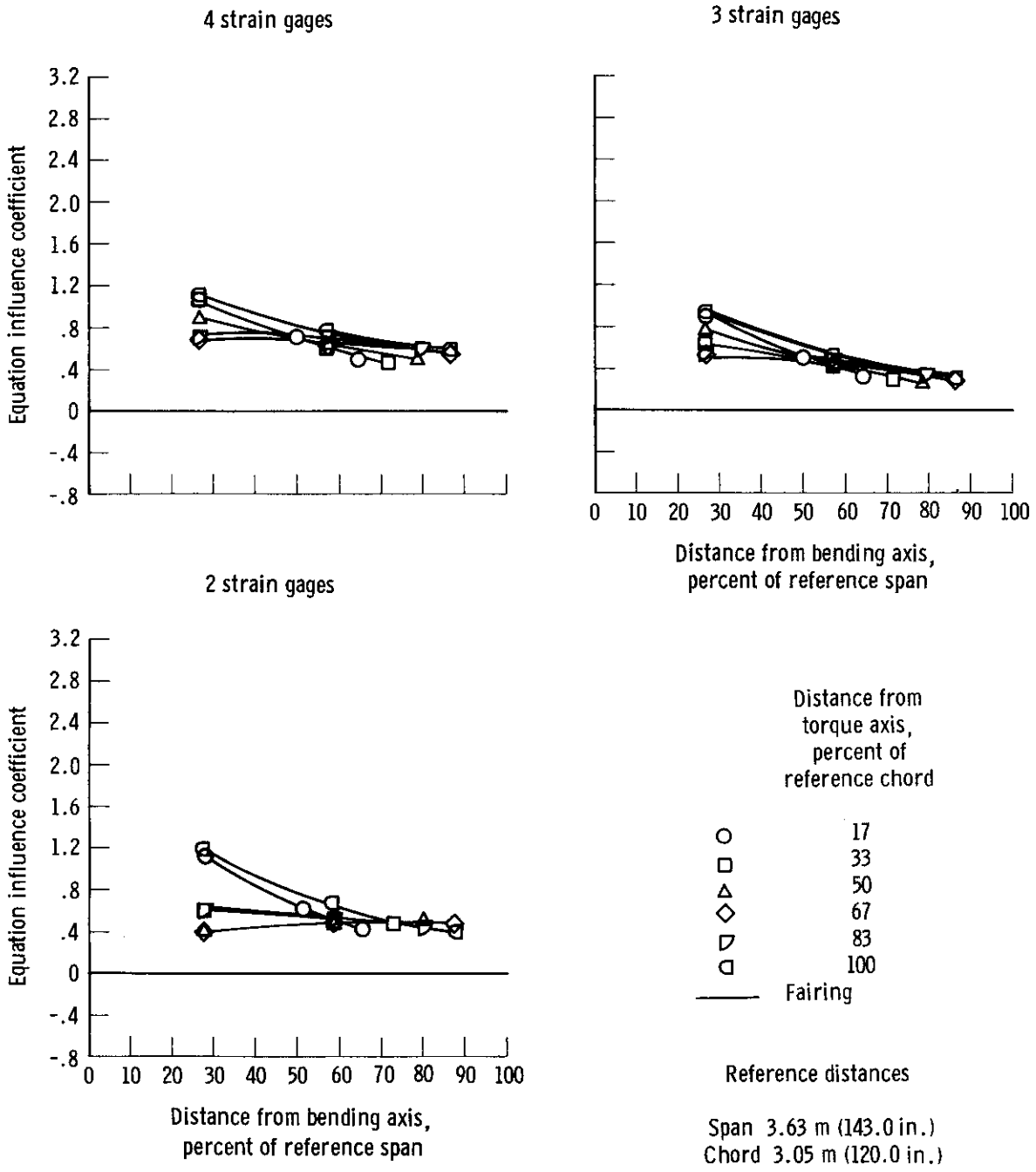

(a) Concluded.

Figure 5. Continued.

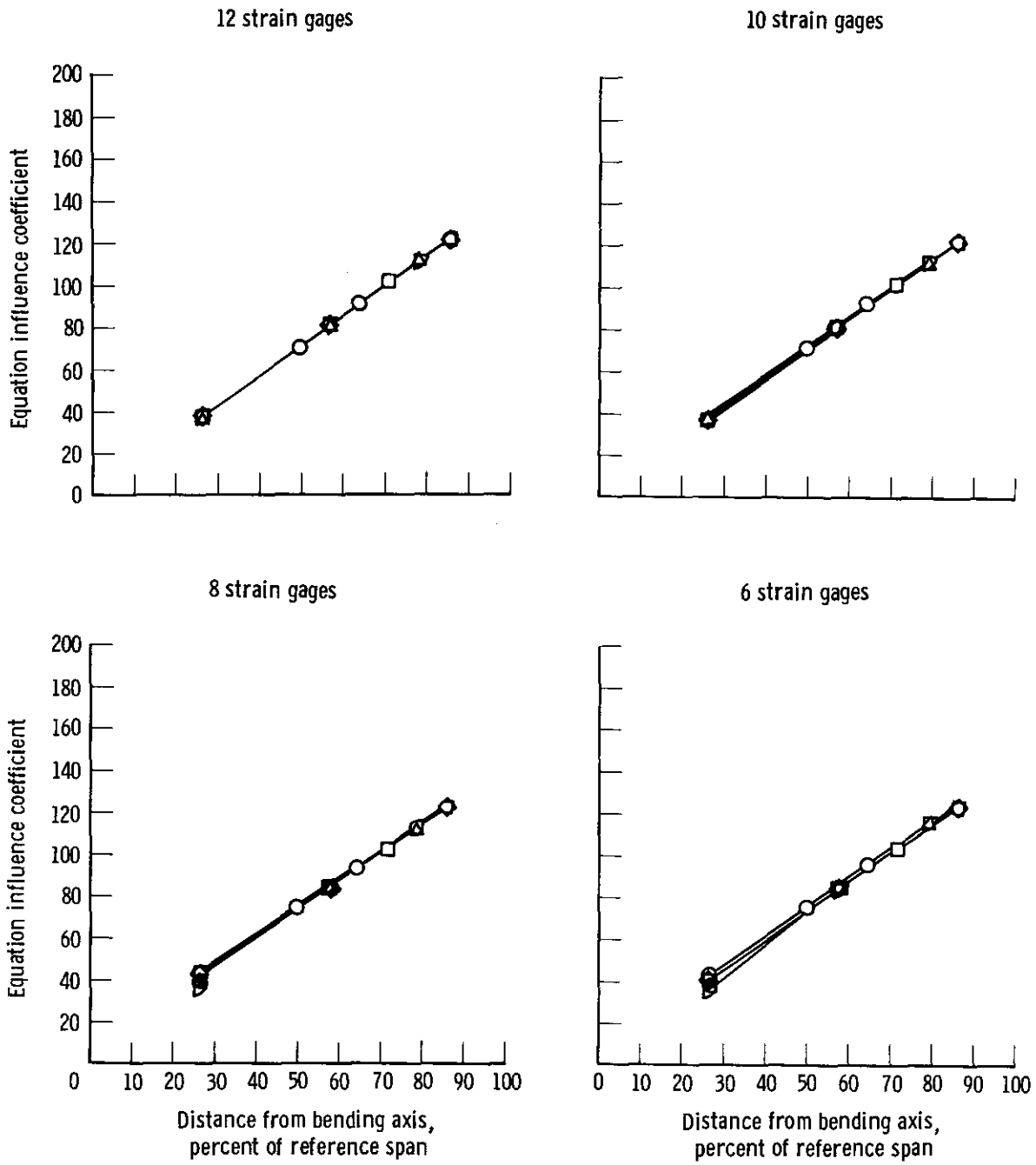

(b) Bending moment.

Figure 5. Continued.

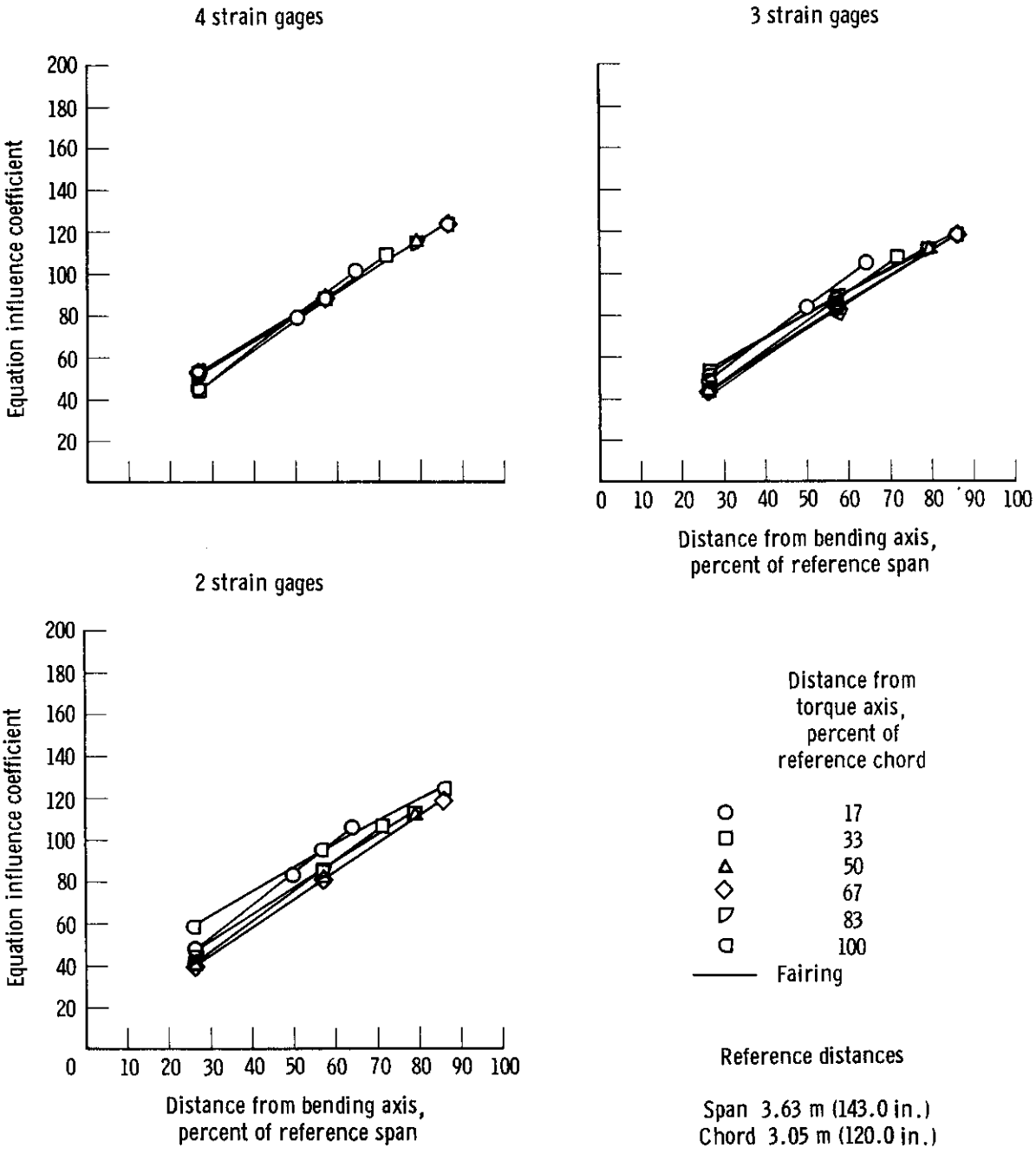

(b) Concluded.

Figure 5. Continued.

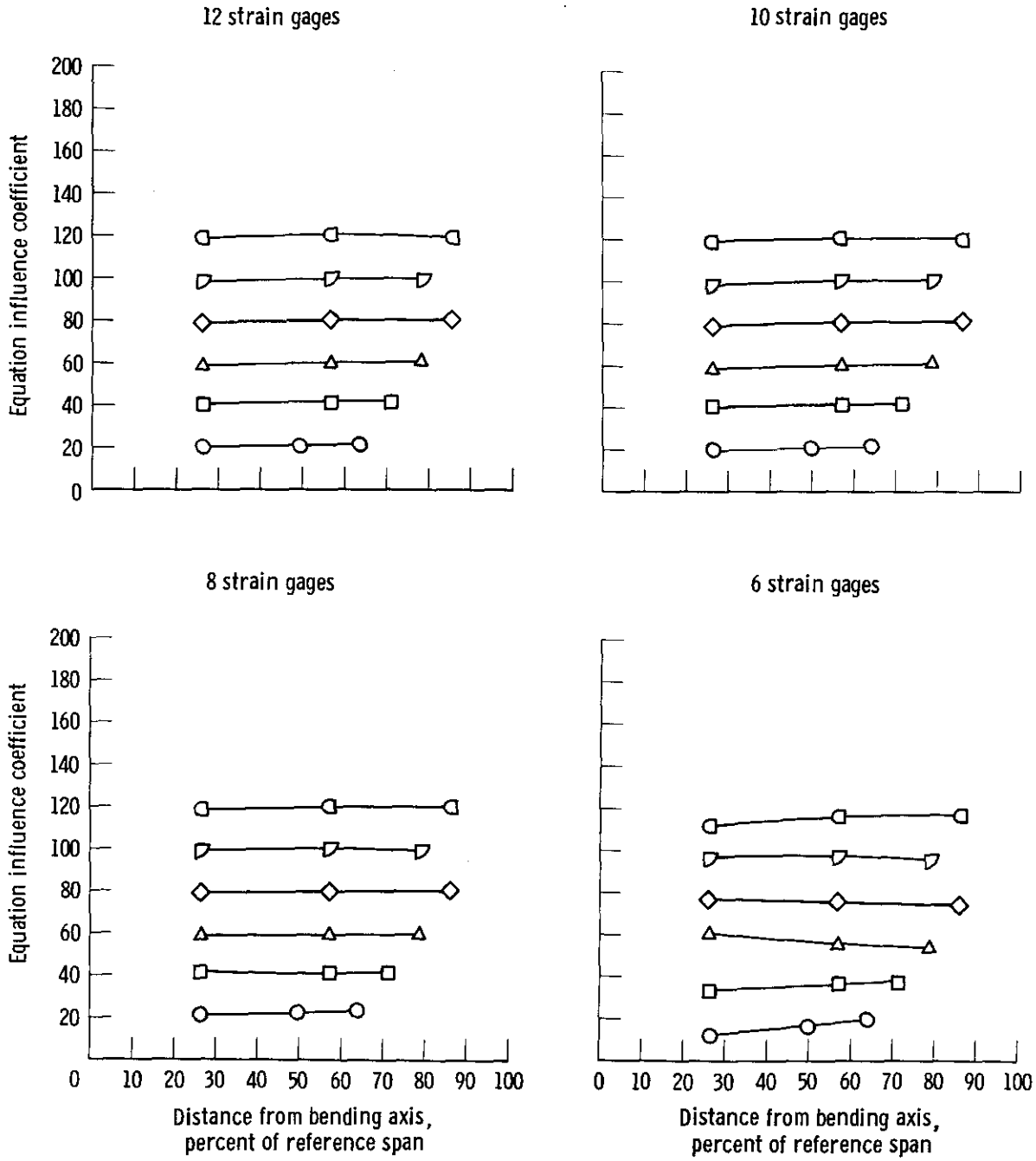

(c) Torque.

Figure 5. Continued.

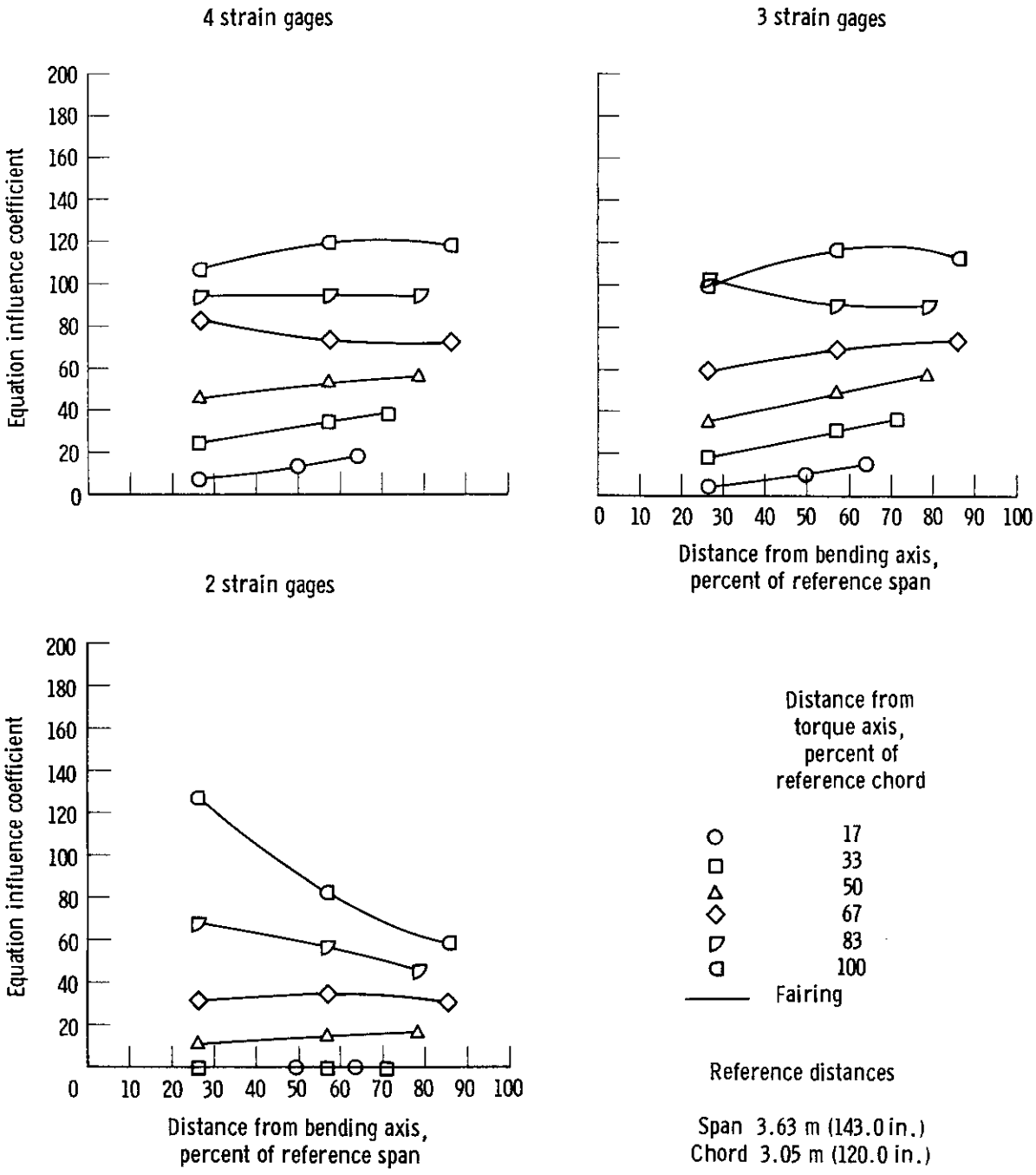

(c) Concluded.

Figure 5. Concluded.

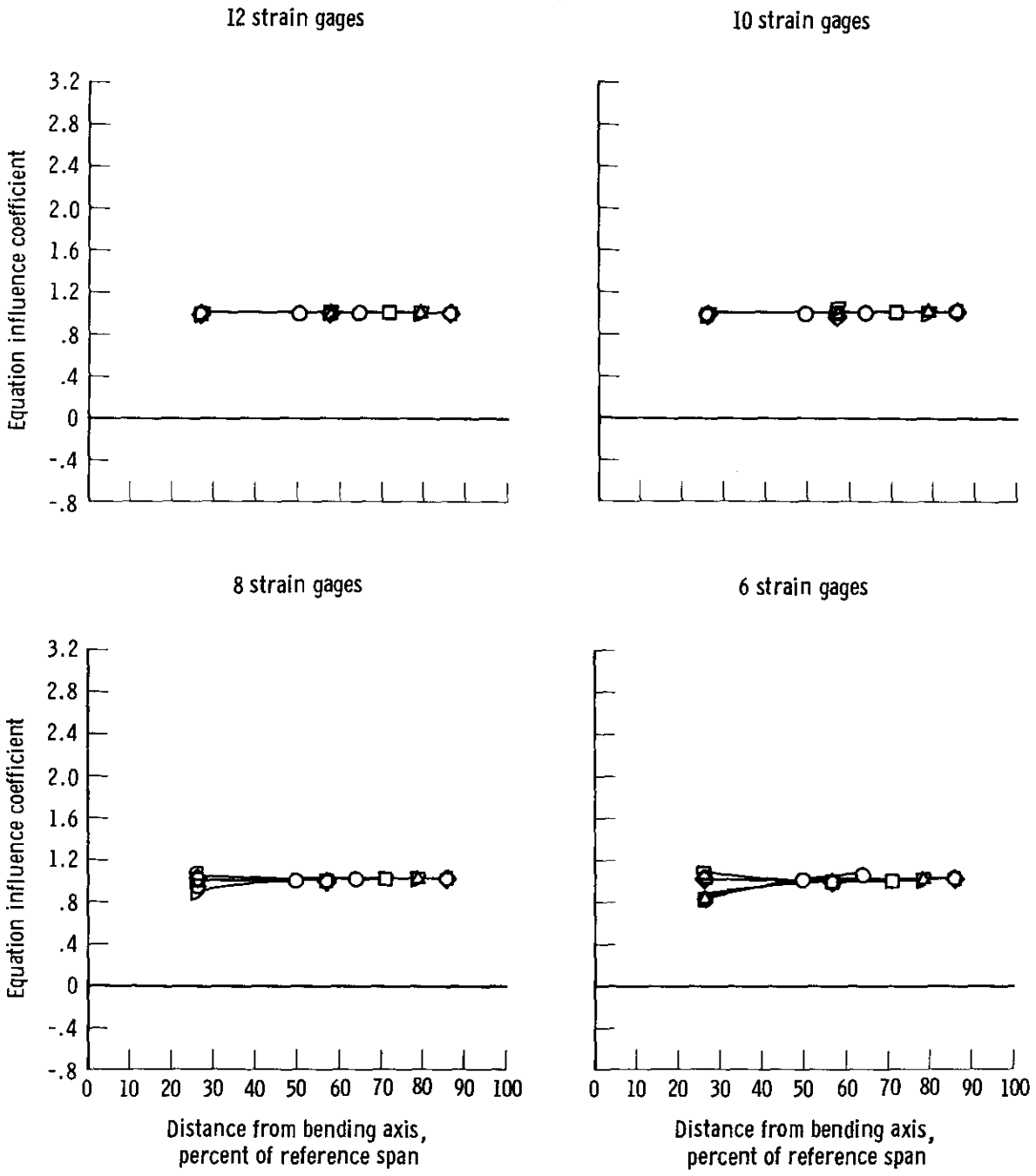

(a) Shear.

Figure 6. MT-value derived equation influence coefficient.

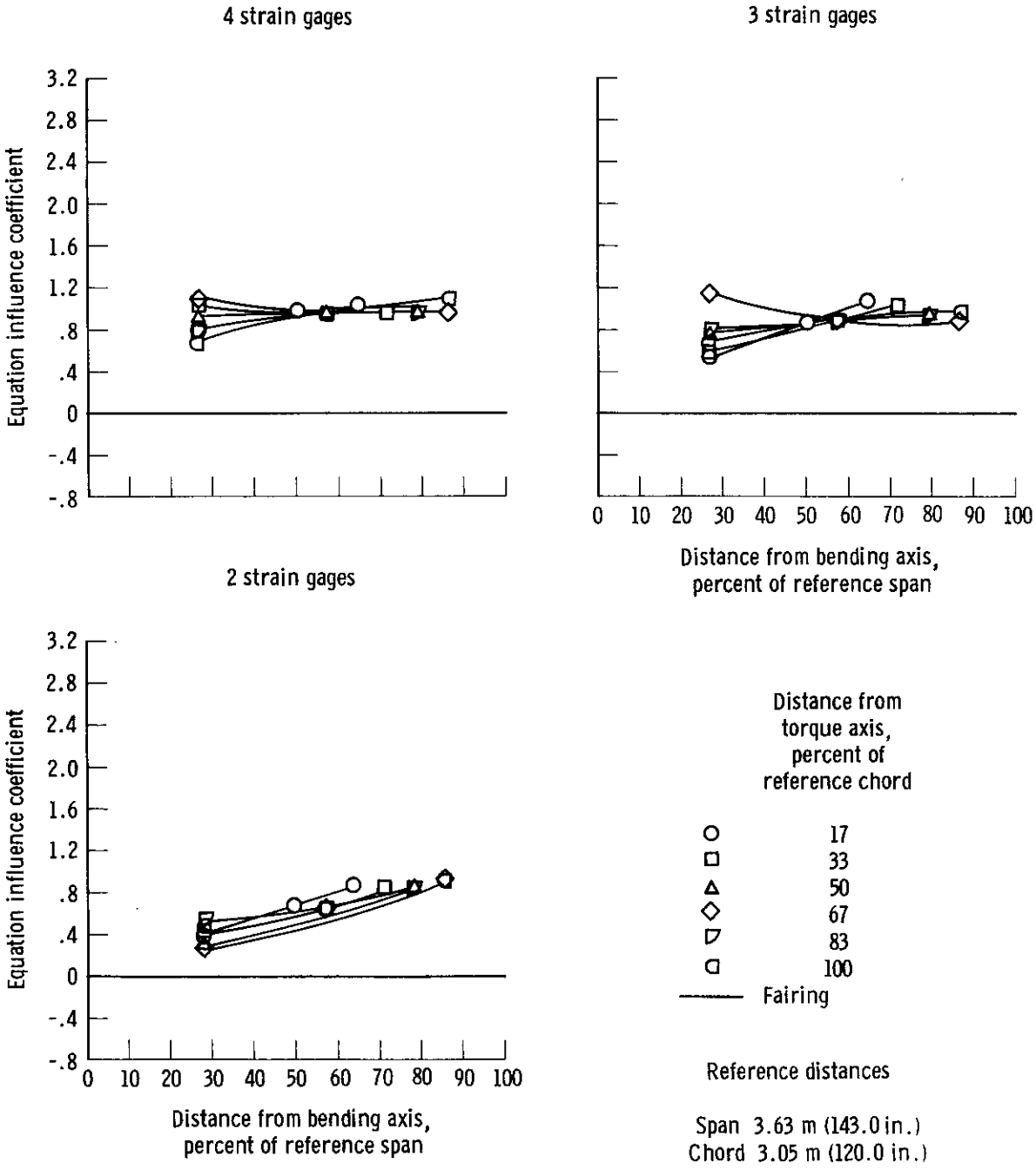

(a) Concluded.

Figure 6. Continued.

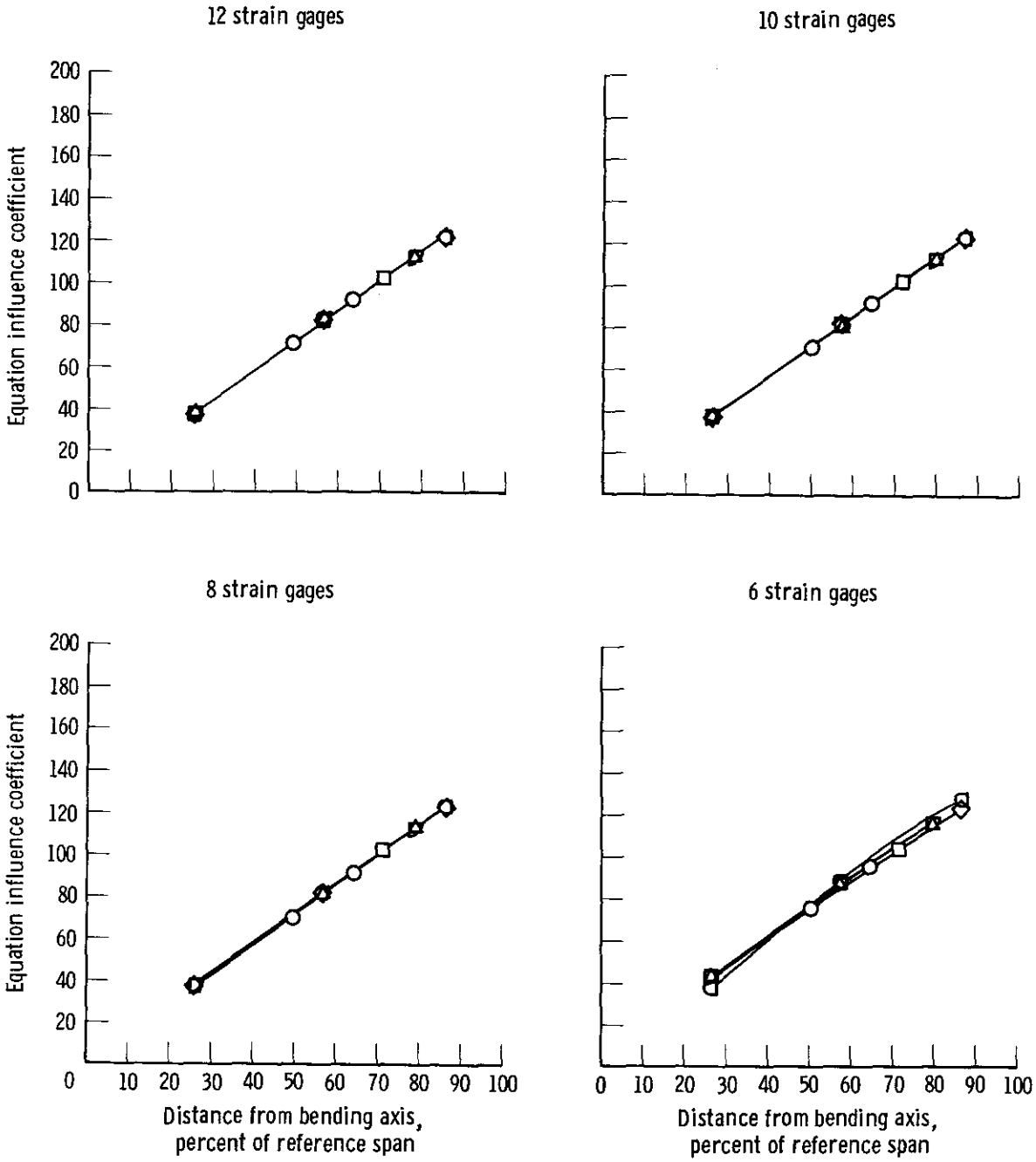

(b) Bending moment.

Figure 6. Continued.

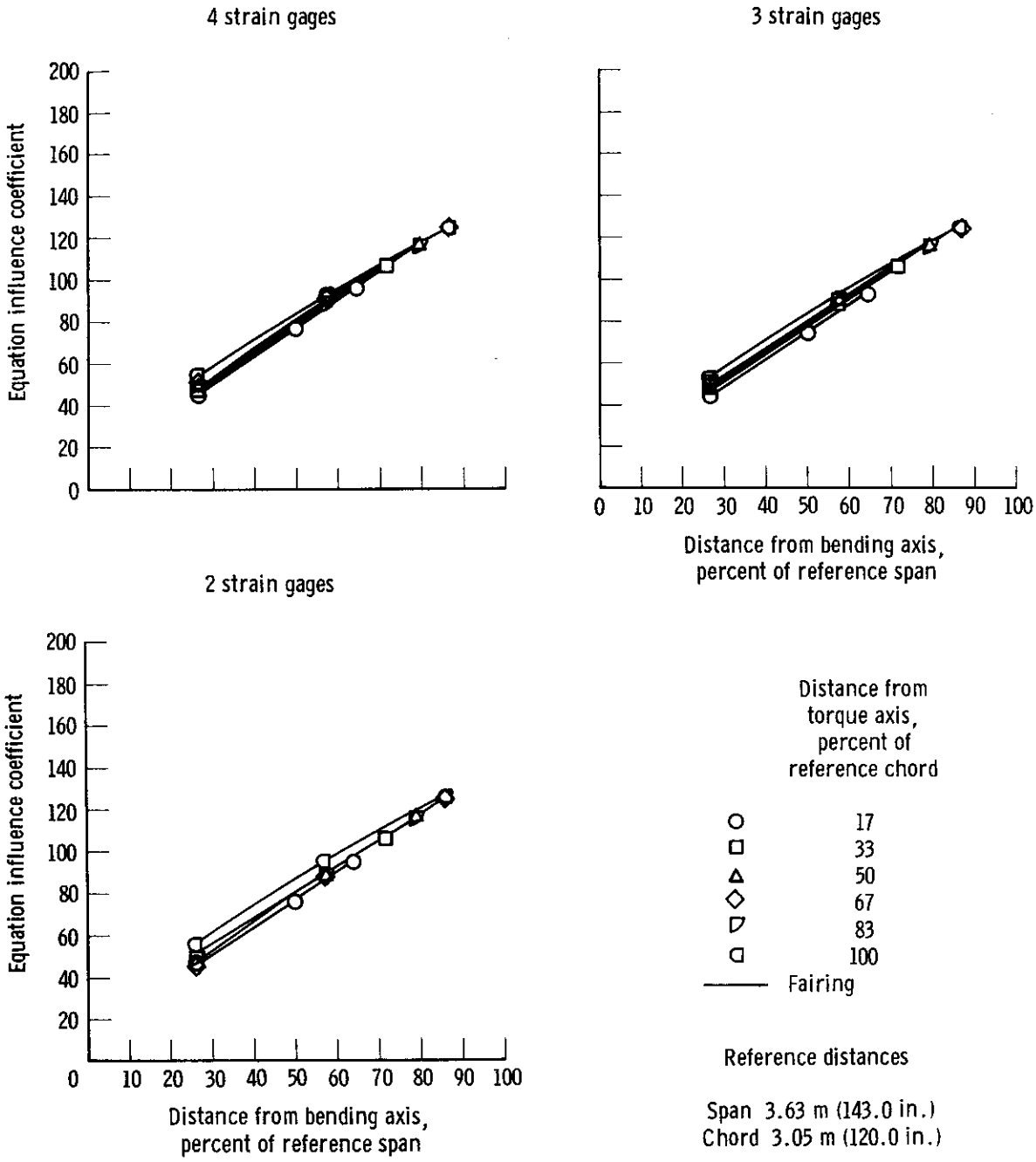

(b) Concluded.

Figure 6. Continued.

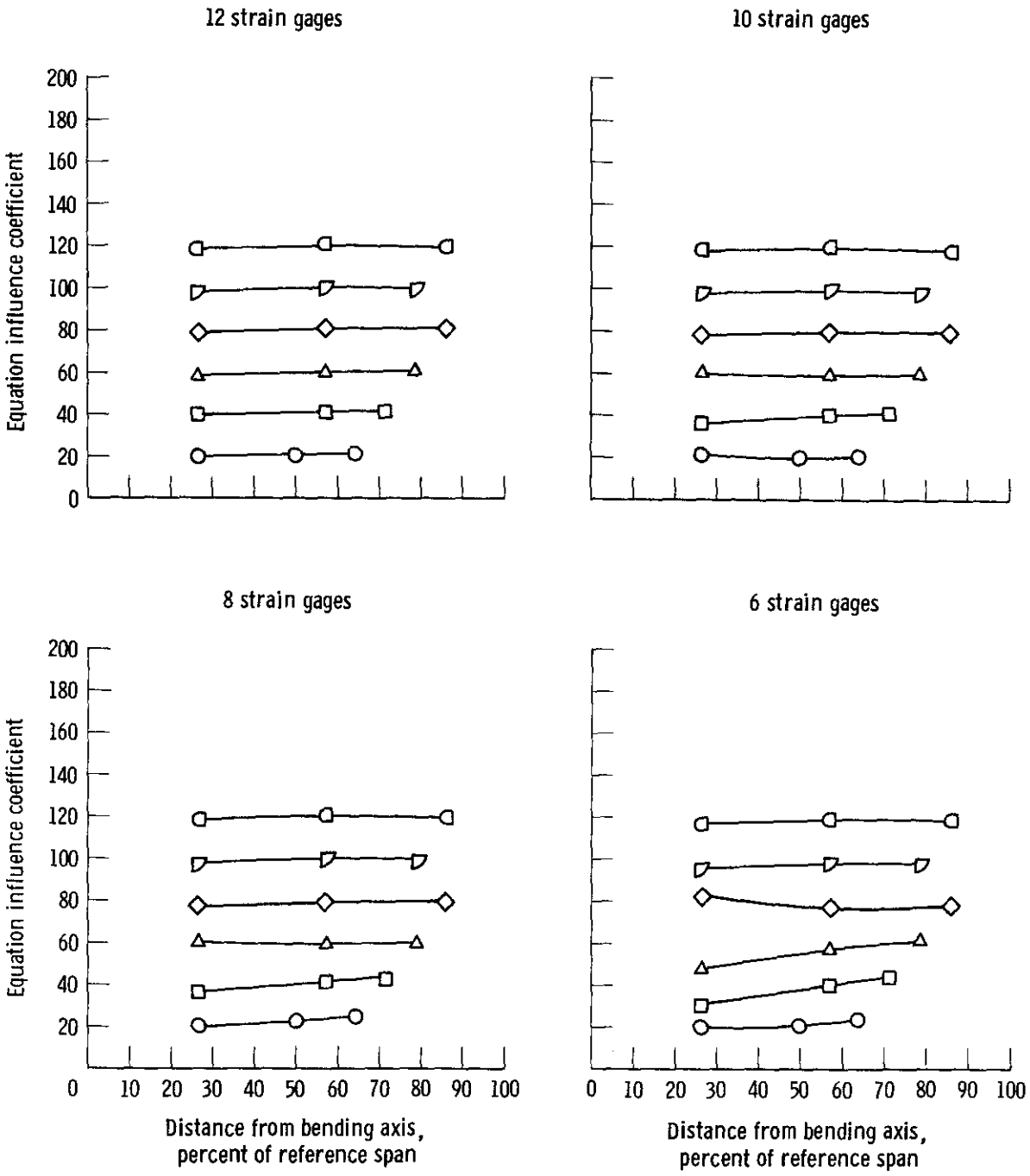

(c) Torque .

Figure 6. Continued.

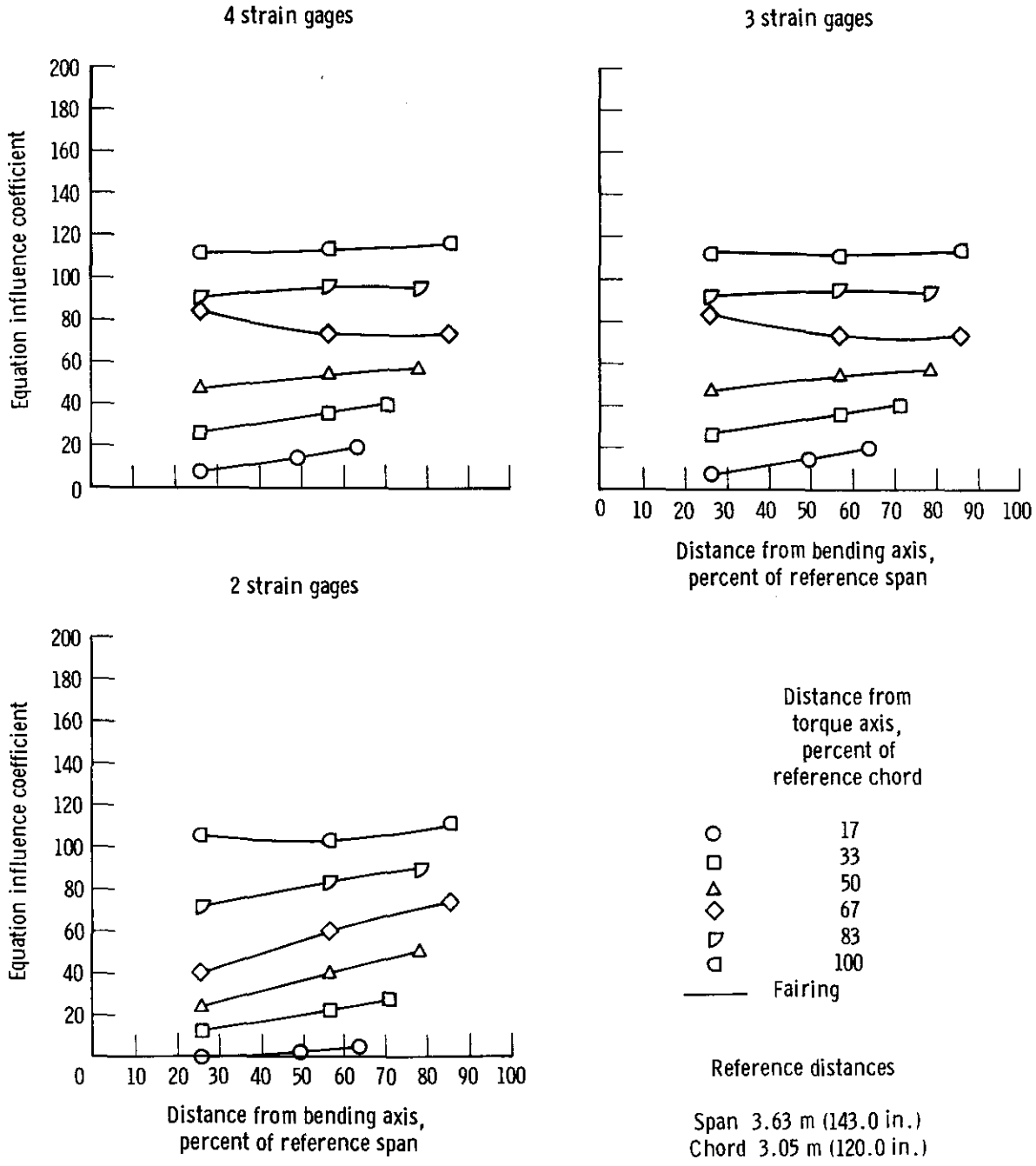

(c) Concluded.

Figure 6. Concluded.

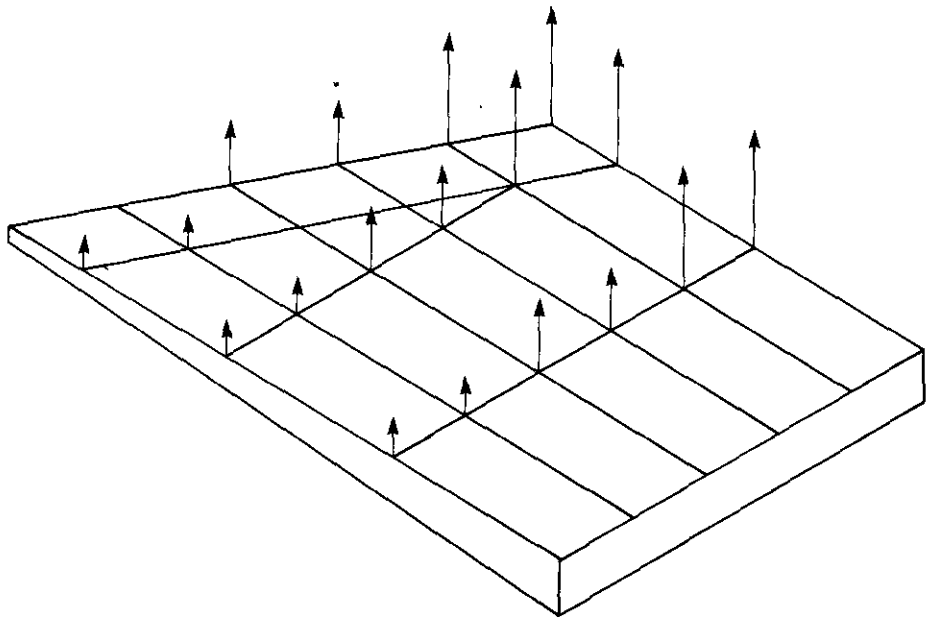

(a) Forward center of pressure representing subsonic flight (48,492 N (10,902 lb)).

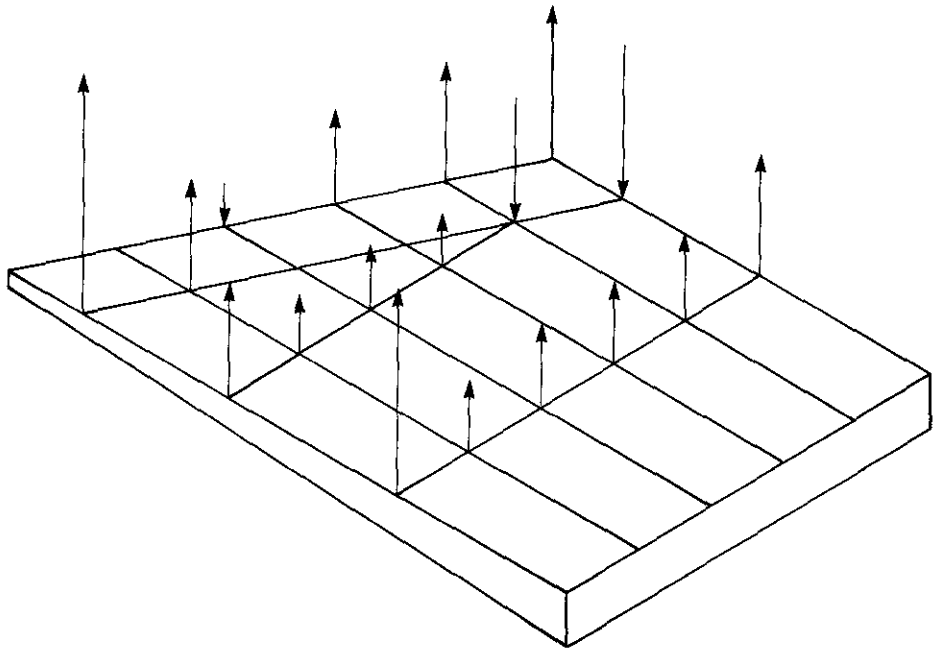

(b) Mid center of pressure representing supersonic flight (88,182 N (19,825 lb)).

Figure 7. Distributed loads used in loads equations.

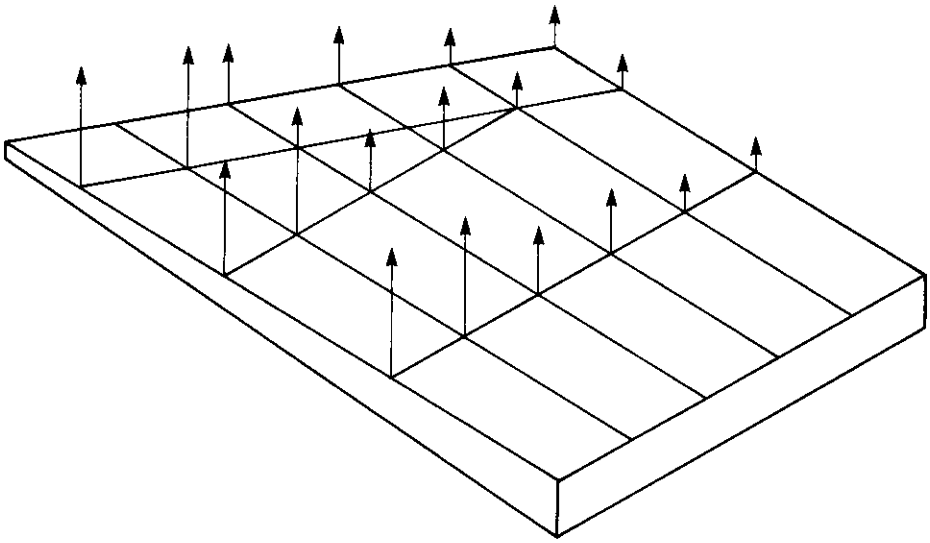

(c) Aft center of pressure representing maneuvering flight (48,252 N (10,848 lb)).

Figure 7. Concluded.

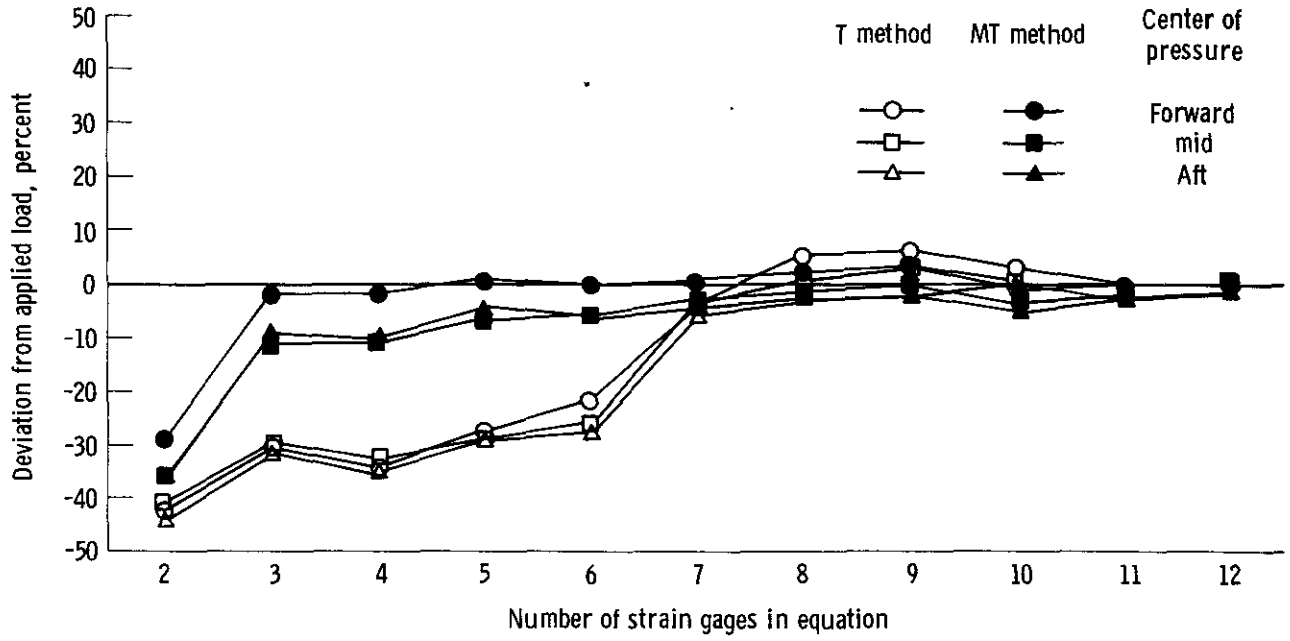

(a) Shear.

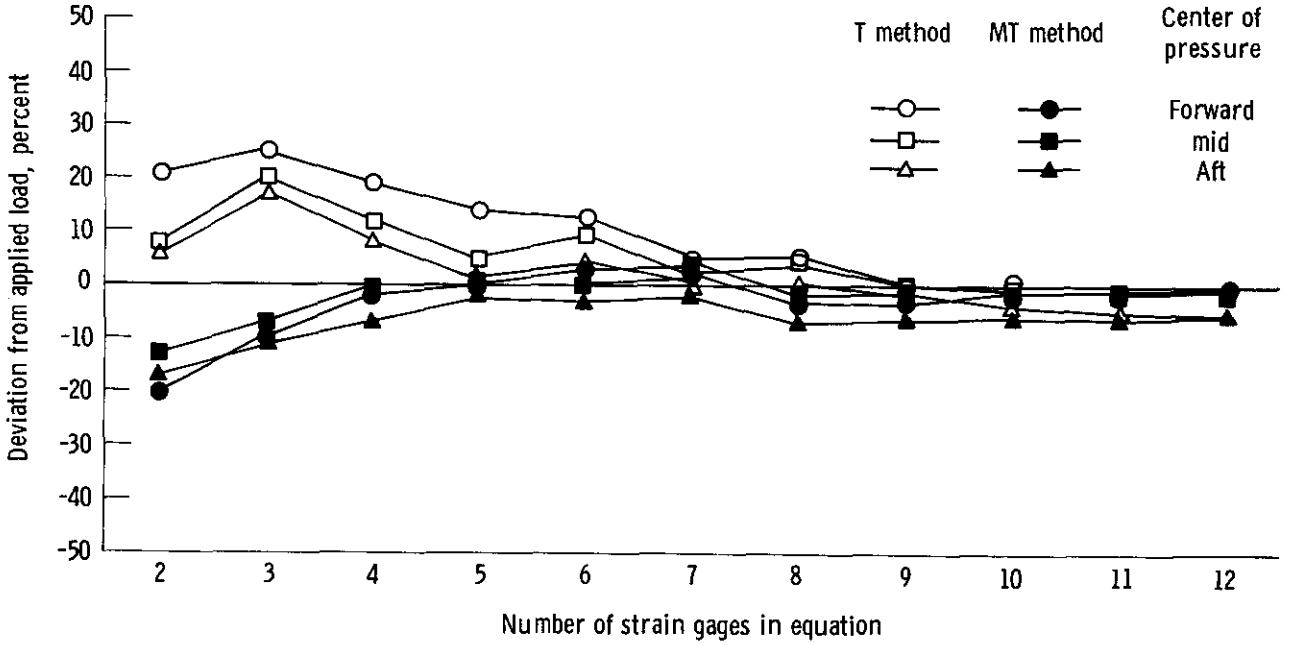

(b) Bending moment.

Figure 8. Comparison of loads computed with T and MT methods.

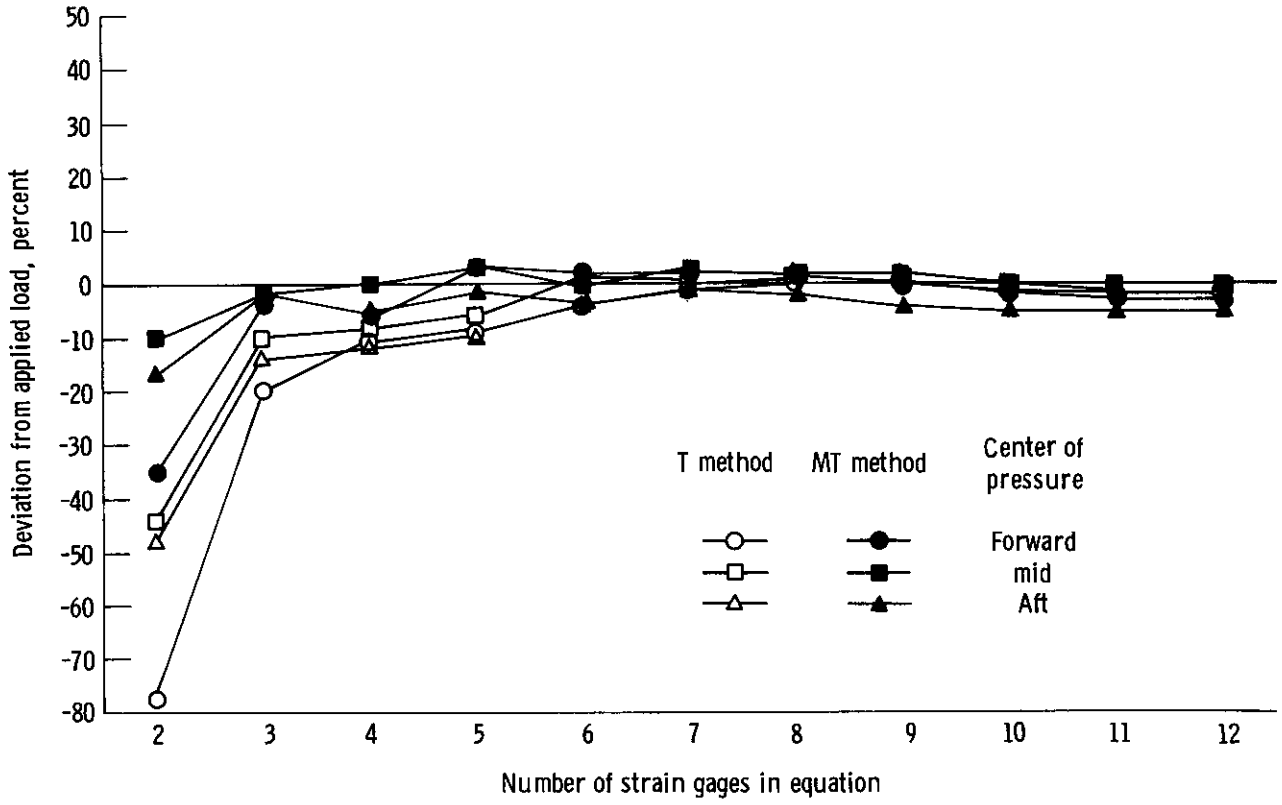

(c) Torque.

Figure 8. Concluded.